

ADVANCED UNDERGRADUATE LABORATORY
TEM
ELECTRON MICROSCOPE

Minor revisions: October 2015 by Peter Krieger
Revised: September 1995 by B.W. Statt

Transmission Electron Microscope

The transmission electron microscope (TEM) is a common tool used by researchers in many fields to study samples on length scales less than an optical wavelength. Until recently it was the only method available for imaging on these length scales. It is widely used in biology and materials science. In both cases real space images are taken and in the latter case diffraction is also performed. This lab concerns itself mostly with diffraction although there is the opportunity to image magnetic domains of nickel.

As a historical note the first electron microscope in North America was built at U of T around 1940. Shortly after that some of those involved were attracted to RCA who then went on to produce commercial units.

The appendix describes in detail how scattering takes place in the sample and how this can be used to determine the crystal structure of your samples. It is important that you master this material in order to understand how the TEM is used in diffraction work. To put it simply though, Bragg's Law is responsible for the diffraction rings observed on the fluorescent screen of the TEM.

EXPERIMENT

1. In this experiment, the diffraction pattern from the small grain Au sample will be used to calibrate the diffraction pattern photographs of other samples.

The lattice structure of Au is f.c.c. and the lattice constant is 4.08Å.

Take a photograph of the ring diffraction pattern from the sample using a suitable accelerating voltage and suitable lens currents. Make sure the diffraction pattern is large enough to be able to measure the ring diameters easily. Using the relationship between the interplanar distance d_{hkl} and the ring diameter D

$$d_{hkl} = n \left(\frac{K}{D} \right) \quad (1)$$

where K is the camera constant and n is an integer, do the following:

- i) Find an approximate value of the camera constant K for the photograph.
- ii) Label each ring with the Miller indices h, k and l of the set of planes that produced it.

- iii) Once you have correctly carried out steps I) and II), you should have an accurate value of d_{hkl} corresponding to each ring of the pattern. Using these values of d_{hkl} , start over and calculate the exact value of the camera constant K for each ring. Plot the value of K as a function of distance from the centre of the diffraction pattern.

Parts (I) and (ii) above will necessarily involve some trial and error fitting of d_{hkl} , n and K values. The graph obtained in part (iii) can be used to get the camera constant K for any diffraction photograph taken under the same conditions (i.e. lens currents, accelerating voltages and aperture settings all the same).

2. Take a photograph of the ring diffraction pattern from the Al sample using the same settings as in section (1) part (iii). Using the calibration curve of section (1), you can now analyze the Al diffraction pattern.

Determine the lattice structure, find the lattice constant a, and label the diffraction rings with the Miller indices of the corresponding lattice planes.

3. Now find the lattice spacing and crystal structure of the "unknown" sample.
4. Now that you are familiar with "powder diffraction" patterns you should now grow an epitaxially oriented film and observe it's diffraction pattern. An epitaxial film can be grown by depositing nickel onto a cleaved surface of a crystal. In this case NaCl is used. Using the evaporator you can deposit a thin film of say 300 Å onto the crystal. Then the film is lifted from the crystal in water and then put onto the usual Cu mesh TEM holder. From the diffraction pattern determine which crystal plane has been grown.
5. If time permits you may want to have a look at domain structures in nickel. The Curie point of pure nickel is at a temperature of $T_c = 627$ K. Again, this is a temperature which is easily attainable with the heating stage of the Hitachi EM III electron microscope. It is possible to photograph the decay of the magnetic domains in a selected field of view as the temperature is raised through the curie temperature T_c . The thermocouple used is not very well thermally connected to the nickel specimen on the heating stage, so that the temperature should be changed as slowly as possible to give the thermocouple some chance of representing the temperature of the nickel. You can estimate the value for T_c from the point at which the magnetic domains vanish. Explain how the domain walls are rendered visible by the TEM.

BASIC OPERATING INSTRUCTIONS

It is advisable to notify Mr. Rob Smidrovskis the day before you want to use the TEM so that he can warm it up early in the morning before you get in. This can save you an hour or two!

To evacuate and turn on the microscope

- i. Turn the fore pump valve to 'L'. This allows the fore pump to pump on the selector valve and the main valve.
- ii. Turn on the fore pump. Switches are on the power supply cabinet and on the mechanical pump.
- iii. Turn the main valve to 'D'. This allows the fore pump to pump out the diffusion pump enclosures. Note that the diffusion pumps are not yet open to the microscope itself.
- iv. Turn the selector valve to 'C'. This allows the fore pump to pump the camera chamber, and hence the interior of the microscope, since the camera chamber air lock is open.
- v. Turn on the water supply. This provides cooling water for the diffusion pumps.
- vi. Turn the diffusion pump on. This switch is on the power supply cabinet. This turns on the heaters in the diffusion pumps.
- vii. Allow 30 minutes for the diffusion pump oil to heat up. Turn the selector valve to 'P' or 'S'. This cuts the fore pump off from the microscope body. The plate reservoir and specimen chamber are not connected to the microscope body in normal operation.
- viii. Then turn the main valve to 'H'. This causes the diffusion pumps to open to the microscope body and pump the microscope interior down to a high vacuum. The fore pump now pumps on the back of the diffusion pumps.
- ix. Before turning on the electron beam, make sure that the vacuum indicator is in the green region.

To change samples

As the microscope can be easily damaged during this procedure, please consult your TA, professor or Mr. Rob Smidrovskis if you have not changed a sample before.

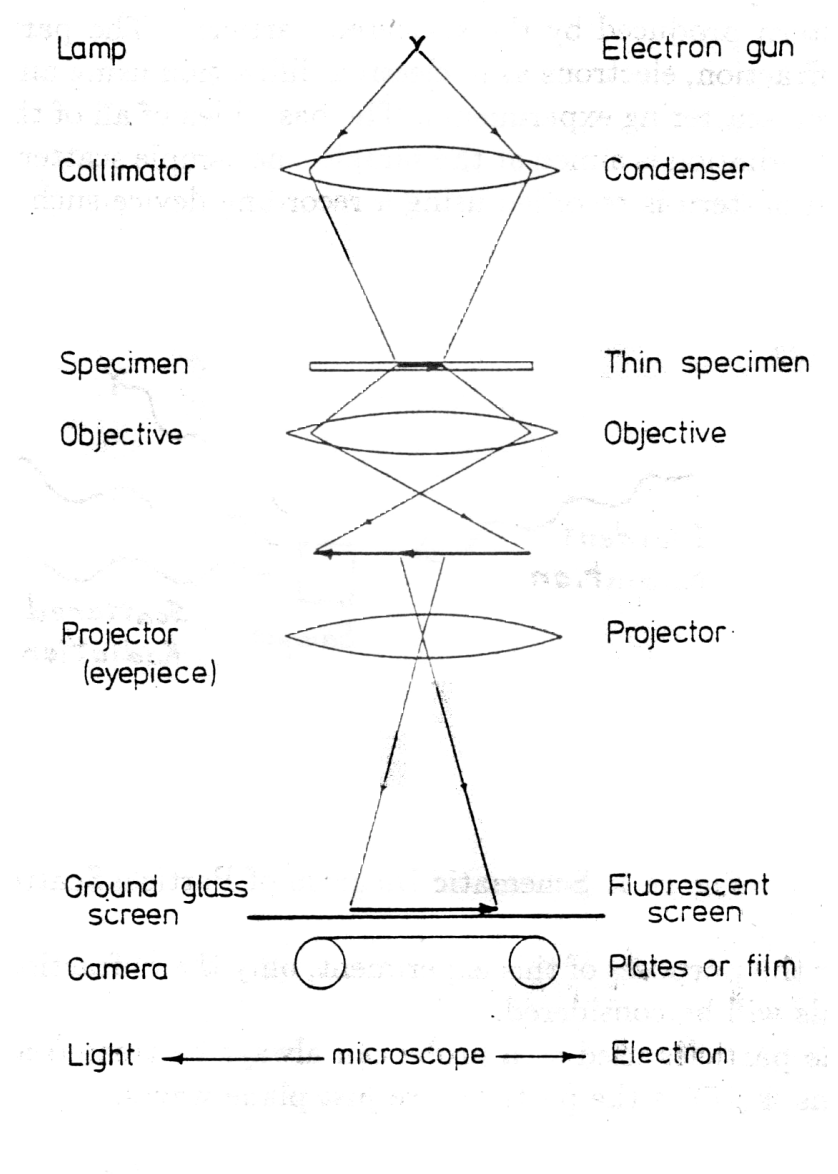
- i. If the filament current is on it must be turned off. Turn the high voltage knob to the voltage setting with filament off (i.e. NOT the 'F' position).
- ii. Turn the selector valve to 'S'. This opens a path from the fore pump valve to the specimen chamber.
- iii. Use the sample transport device to pick up the sample from the microscope specimen stage, and bring the sample and holder into the specimen chamber. The sample holder chamber should be lined up with the round window of the specimen chamber. In this position the specimen chamber is isolated from the microscope interior.
- iv. Turn the form pump valve to 'A'. This allows air into the specimen chamber.
- v. The plexiglass window of the specimen chamber can now be removed and the samples changed.
- vi. Replace the specimen chamber window and turn the fore pump valve to 'L'. This allows the fore pump to pump out the specimen chamber.
- vii. When the fore pump has stopped gurgling, use the sample transport device to place the new sample in the microscope specimen stage.
- viii. Make sure the transport device is returned to its original position in the sample chamber. Otherwise the mechanism will interfere with the electron beam.

To turn off the microscope

- i. Turn the main valve to 'D'. This cuts off the diffusion pump and fore pump from the microscope interior.
- ii. Turn the diffusion pump switch on the power supply cabinet. This turns off the heaters in the diffusion pumps.
- iii. Allow 30 minutes for the diffusion pump oil to cool down. Then turn the main valve to 'OFF', the selector valve to 'OFF' and pull the locking pin of the fore pump valve and turn it to 'S'.
- iv. Turn off the vacuum gauges, the fore pumps and the main power switches.

To operate the microscope

Consult the manuals, your TA, professor or Mr. Rob Smidrovskis for instructions on how to operate the controls of the microscope. The following diagram illustrates the basic operation of the microscope by analogy to an optical microscope.



Comparison of optical and TEM microscopes

APPENDIX

Scattering from Crystals and the Reciprocal Lattice

The most common method of obtaining information about atomic arrangements in solids, liquids and gases is to scatter particles from the material under study and observe the diffraction pattern produced by the scattered particles. The particles used can be photons as in x-ray diffraction, electrons as in electron diffraction using an electron microscope, or neutrons in neutron scattering experiments. The basic idea of all of these methods is exactly the same. Incident radiation is aimed at the sample, the sample scatters the radiation, and the scattered radiation pattern is recorded using a recording device such as photographic film.

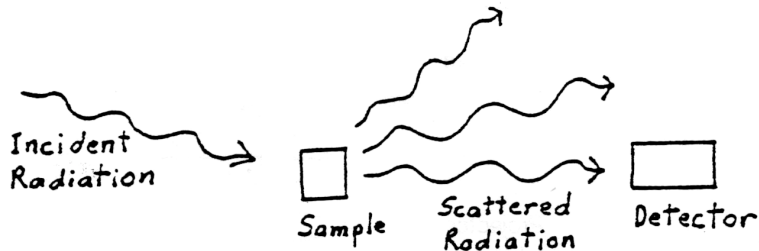


Figure 1: Schematic Diagram of Particle Scattering from a Sample.

For the purposes of this experiment, only the diffraction pattern produced by crystalline materials will be considered.

The particles used as a probe can always be treated as free particles. Hence the wave functions $\Psi_k(\vec{r})$ of the particles are just plane waves.

$$\Psi_k(\vec{r}) = A e^{i\vec{k} \cdot \vec{r}} \quad (1)$$

where \vec{k} is the particle wave vector.

Recall that the particle momentum is $\hbar\vec{k}$, the wavelength λ is $\frac{2\pi}{|\vec{k}|}$, and the energy is $\frac{\hbar^2 k^2}{2m}$.

To a good approximation, the scattering of the probe particles by atoms of a crystal is elastic. Therefore if \vec{k} is the wave vector of an incident particle and \vec{k}' the wave vector of the particle after scattering, the condition $|\vec{k}| = |\vec{k}'|$ must hold.

The scattering of a particle from state $\Psi_k(\vec{r})$ to the state $\Psi'_k(\vec{r})$ by a crystal can be represented by the vector diagram in \vec{k} -space shown in figure 2.

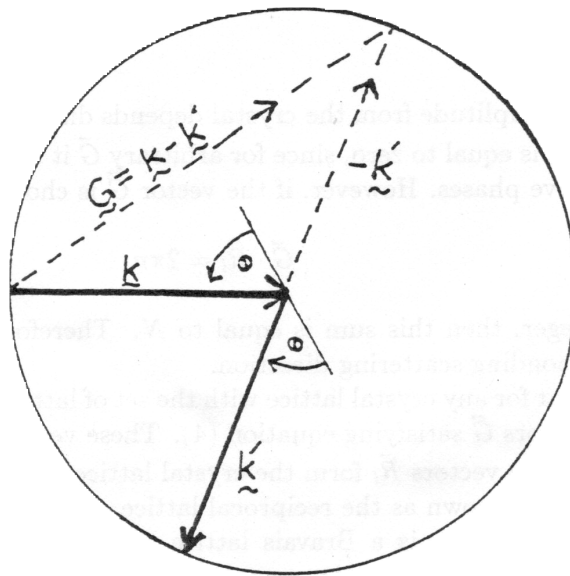


Figure 2: Scattering Diagram in \vec{k} -space.

The sphere is the locus of all scattered vectors \vec{k}' which satisfy the condition $|\vec{k}| = |\vec{k}'|$. This sphere is known as the Ewald sphere. The difference vector \vec{G} turns out to be the important quantity in interpreting the diffraction patterns produced by a crystal. The angle θ is the scattering angle (i.e. the 'grazing' angle between the vectors \vec{k} or \vec{k}' , representing the incident or scattered beam directions, and the 'scattering plane' of atoms in the crystal).

The crystal lattice can be represented by a set of N vectors in real space. These are denoted by \vec{R}_l for $l = 1$ to N . \vec{R}_l is the vector from some origin to the l^{th} lattice site. The vectors are of the form

$$\vec{R}_l = n\vec{a} + m\vec{b} + p\vec{c} \quad (2)$$

where n, m and p are integers and the vectors \vec{a} , \vec{b} and \vec{c} are the basis vectors of the lattice site.

Now we suppose a plane wave of the form $e^{i\vec{k}\cdot\vec{r}}$ representing a particle in the state $\Psi_k(\vec{r})$ is incident upon the lattice. The phase of the wave at the l^{th} lattice site is $\vec{k} \cdot \vec{R}_l$. A detector is placed at some position \vec{r}' very far from the crystal compared to the interatomic spacing. If \vec{k}' is the wave vector of the wave scattered in the direction of \vec{r}' from the l^{th} crystal lattice site, the phase of the scattered wave at \vec{r}' will be $\vec{k} \cdot \vec{R}_l + \vec{k}' \cdot (\vec{r}' - \vec{R}_l)$. That is, the total phase at \vec{r}' is the phase at the l^{th} lattice site plus the phase change of the wave in travelling from \vec{R}_l to \vec{r}' .

The total scattered amplitude at \vec{r}' is the sum of the scattered wave contributions from each lattice site \vec{R}_l .

$$A(\vec{r}') = \sum_l e^{i(\vec{k} \cdot \vec{R}_l + \vec{k}' \cdot (\vec{r}' - \vec{R}_l))} = e^{i\vec{k}' \cdot \vec{r}'} \sum_l e^{i(\vec{k} - \vec{k}') \cdot \vec{R}_l} = e^{i\vec{k}' \cdot \vec{r}'} \sum_l e^{i\vec{G} \cdot \vec{R}_l} \quad (3)$$

where $\vec{G} = \vec{k} - \vec{k}'$.

The scattering amplitude from the crystal depends directly on the lattice sum $\sum_l e^{i\vec{G} \cdot \vec{R}_l}$. In general, this sum is equal to zero, since for arbitrary \vec{G} it is just the superposition of waves with random relative phases. However, if the vector \vec{G} is chosen such that

$$\vec{G} \cdot \vec{R}_l = 2\pi n \quad (4)$$

where n is an integer, then this sum is equal to N. Therefore, there will be a very bright spot in the corresponding scattering direction.

It turns out that for any crystal lattice with the set of lattice vectors \vec{R}_l , there corresponds a discrete set of vectors \vec{G} satisfying equation (4). These vectors \vec{G}_i form a lattice in \vec{k} -space in the same way as the vectors \vec{R}_l form the crystal lattice in real space. This abstract lattice in wave vector space is known as the reciprocal lattice.

If the real space lattice is a Bravais lattice with basis vectors \vec{a} , \vec{b} and \vec{c} , it follows immediately that the reciprocal lattice vectors \vec{G}_i can be constructed from the basis vectors \vec{u} , \vec{v} and \vec{w} given by the formulas in equation (5).

$$\vec{u} = 2\pi \frac{(\vec{b} \times \vec{c})}{\vec{a} \cdot (\vec{b} \times \vec{c})} \quad (5a)$$

$$\vec{v} = 2\pi \frac{(\vec{c} \times \vec{a})}{\vec{a} \cdot (\vec{b} \times \vec{c})} \quad (5b)$$

$$\vec{w} = 2\pi \frac{(\vec{a} \times \vec{b})}{\vec{a} \cdot (\vec{b} \times \vec{c})} \quad (5c)$$

Because \vec{u} , \vec{v} and \vec{w} depend on the real space basis vectors \vec{a} , \vec{b} and \vec{c} in the above manner, the reciprocal lattice corresponding to a given crystal is determined by the crystal lattice in terms of both orientation and lattice structure. Hence the importance of the concept of a reciprocal lattice. If we know the reciprocal lattice of a crystal we can work backwards to find both the orientation of the crystal lattice as well as the lattice structure.

It was shown above that the peaks in the diffraction pattern produced by radiation scattering from a crystal occur when the difference wave vector \vec{G} is a reciprocal lattice vector. The diffraction pattern produced by a crystal is then a direct picture of a crystal's reciprocal lattice and so yields a great deal of structure and orientation information about the crystal.

It is at this point that the Ewald sphere construction of figure 2 becomes useful. If figure 2 is superposed over the reciprocal lattice of the scattering crystal so that the origins of the Ewald sphere and the reciprocal lattice coincide, the diagram in figure 3 results.

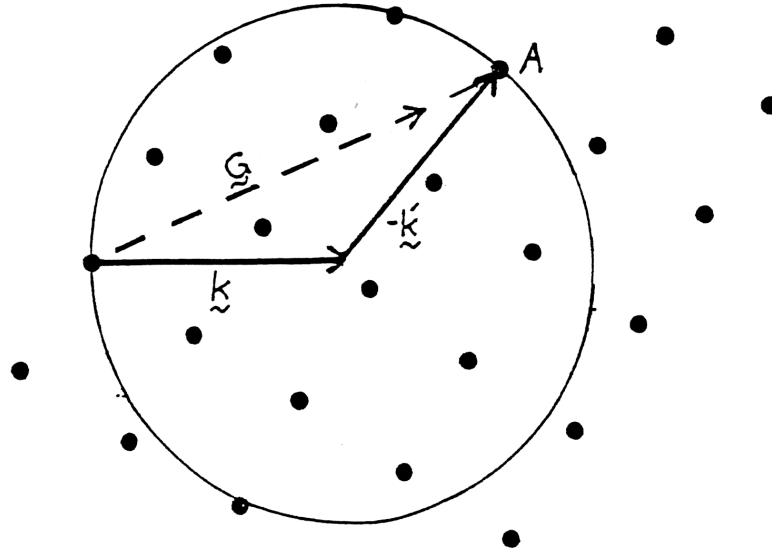


Figure 3: Superposition of the Ewald Sphere on the Reciprocal Lattice.

The dots are the lattice points of the reciprocal lattice and the focus of all possible \vec{G} vectors forms the Ewald sphere. Because a diffraction peak results only when \vec{G} is a reciprocal lattice vector, only those reciprocal lattice points lying on the Ewald sphere will produce a diffraction spot in the direction of \vec{k}' . This is how a spot pattern is produced by single crystal scattering.

If instead of using a single crystal, the scattering is from many crystals all oriented randomly with respect to each other, a different diffraction pattern will result. Scattering from a large number of randomly oriented crystals is equivalent to scattering from a single crystal while it is rotated through all possible angles. The reciprocal lattice in figure 3 is then also rotated through all possible angles, keeping the point at the origin fixed. The focus of points where a given reciprocal lattice point, say the one at A in figure 3, intersects the Ewald sphere will be a circle perpendicular to the incident wave vector \vec{k} . Thus any scattering direction of \vec{k}' such that \vec{G} lies on this circle will produce a diffraction peak. It follows that the diffraction pattern produced by the reciprocal lattice point at A will be a cone such that the angle between \vec{k} and \vec{k}' is constant. The total diffraction pattern from a large number of randomly oriented crystals will be a set of cones in wave vector space. If one were to put a photographic plate to the right of figure 3, the cones would intersect the photographic plate to form rings. This is how a ring diffraction pattern is produced.

To see why scattering experiments using an electron microscope differ from those using x-rays, it is necessary to look at the relative scales of the Ewald circle and the reciprocal lattice spacing in wave vector space. From equations

(5) for the reciprocal lattice wave vectors, the spacing between reciprocal lattice points is of the order of $2\pi/a$ where a is the real space lattice constant. For a typical metal such as Au, a is 4.08\AA . The lattice constant of the reciprocal lattice is then roughly 1\AA^{-1} to 2\AA^{-1} .

Recall that the wave vector \vec{k} is given by $2\pi/\lambda$ where λ is the wavelength of the radiation. For x-ray scattering, λ is of the order of 1\AA , so \vec{k} is of the order of 6\AA^{-1} in length. Because the incident wave vector \vec{k} and the scattered wave vector \vec{k}' are the same length, the radius of the Ewald sphere is also of the order of 6\AA^{-1} . The Ewald sphere and the reciprocal lattice presented in figure 3 are therefore drawn to more or less the right proportions for x-ray scattering.

If an electron microscope is used for scattering experiments, the situation is very different. If a 100 KeV accelerating potential is used to produce the beam of electrons, the electron wavelength is 0.037\AA . The Ewald sphere radius is then $2\pi/0.037 = 161\text{\AA}^{-1}$ which is two orders of magnitude larger than the typical reciprocal lattice spacing. The Ewald sphere diagram must then be redrawn to show the relative sizes of the sphere and the reciprocal lattice. Since in an electron microscope the electrons observed are scattered in the extreme forward direction, only the forward direction of the Ewald sphere is shown in figure 4.

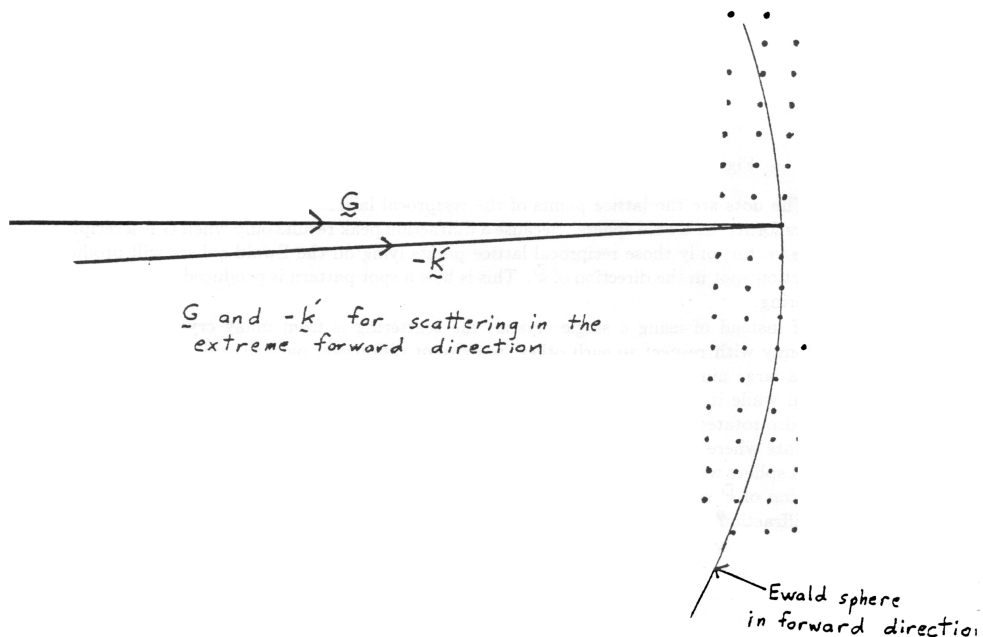


Figure 4: Ewald Sphere and Reciprocal Lattice for Electron Scattering.

In this diagram, the reciprocal lattice points which intersect the sphere tend to lie only on one plane of the reciprocal lattice. The diffraction pattern

produced is an image of this plane. Because the scattering angles are so small, the projection of this diffraction pattern on a film plate retains the spatial relationships between reciprocal lattice points in a given plane.

The plane of the reciprocal lattice that is observed can be chosen by selecting a crystal of the appropriate orientation.

By looking at the diffraction patterns due to several crystal orientations, the reciprocal lattice of the material can be constructed. Using this information, the structure of the crystal in real space can be completely specified.

FUNDAMENTALS OF TRANSMISSION ELECTRON MICROSCOPY

by R. D. Heidenreich

Table C-2

Element	Structure	Lattice Constant			Temperature	Closest Distance	Ionic Radii	Density	Atomic Number Weight	
		a	b	c or Axial Angle						
Aluminum	FCC A1	4.0496			20°C	2.862	Al^{+3} 0.50	2.702	13	26.98
Antimony	Rhombic A7	4.5067		57°6.5'	20°C	2.903	Sb^{+3} 0.90	6.62	51	121.75
Arsenic	Rhombic A7	4.1313		54°10'	20°C	2.51	As^{+3} 0.69	5.727	33	74.92
Barium	BCC A2	5.019			20°C	4.35	Ba^{+2} 1.35	3.5	56	137.34
Beryllium	HCP A3	2.2854		3.584	20°C	2.225	Be^{+2} 0.31	1.85	4	9.02
Bismuth	Rhombic A7	4.746		57°14.2'	20°C	3.111	Bi^{+3} 1.20	9.8	83	208.98
Boron	Rhombic	9.45		23.8	20°C		B^{+3} 0.20	2.34	5	10.81
Bromine	Orthorhombic	4.49	6.68	8.74	-150°C	2.27	Br^{-1} 1.95	3.12	35	79.91
Cadmium	HCP A3	2.979		5.617	20°C	2.98	Cd^{+2} 0.97	8.65	48	112.40
Calcium α	FCC A1	5.582			20°C	3.94	Ca^{+2} 0.99	1.55	20	40.08
* Calcium γ	BCC A2	4.486			500°C	3.88				
Carbon (diamond)	DC A4	3.568			18°C	1.544	C^{+4} 0.15	3.51	6	12.01
graphite	Hex. A9	2.461		6.701	20°C	1.42		2.26		
amorphous								1.8-2.1		
Cerium	FCC A1	5.161			20°C	3.64	Ce^{+3} 1.11	6.67	58	140.12
Cerium	HCP A3	3.62		5.99		3.62	Ce^{+4} 1.01			
Cesium	BCC A2	6.079			-173°C	5.25	Cs^{+1} 1.69	1.90	55	132.91
Chlorine	Tet.	8.58		6.13	-110°C	1.88	Cl^{-1} 1.81	1.56	17	35.45
Chromium	BCC A2	2.885			20°C	2.498	Cr^{+3} 0.69	7.19	24	52.00
* Cobalt α	HCP A3	2.505		4.089	20°C	2.506	Co^{+2} 0.78	8.9	27	58.93
Cobalt β	FCC A1	3.544				2.511	Co^{+3} 0.63			
Columbium (see niobium)										
7 Copper	FCC A1	3.615			20°C	2.556	Cu^{+} 0.98	8.96	29	63.57
							Cu^{+3} 0.69			

USEFUL CRYSTALLOGRAPHIC DATA (Appendix C)

368

FUNDAMENTALS OF TRANSMISSION ELECTRON MICROSCOPY

Table C-2. (Contd.)

Element	Structure	Lattice Constant			Temperature	Closest Distance	Ionic Radii	Density	Atomic Number Weight	
		a	b	c or Axial Angle						
Dysprosium	HCP A3	3.59		5.648	20°C	3.506	Dy^{+3} 0.99	8.54	66	162.50
Erbium	HCP A3	3.559		5.59	20°C	3.466	Er^{+3} 0.96	9.05	68	167.26
Europium	BCC A2	4.606			20°C	3.989	Eu^{+3} 21.12	5.26	63	151.96
Fluorine							F^{-1} 1.36	9	18.99	
Gadolinium	HCP A3	3.636		5.783	20°C	3.561	Gd^{+3} 1.02	7.89	64	157.25
Gallium	FC orthorhombic All	4.52	7.66	4.526	20°C	2.442	Ga^{+3} 0.62	5.91	31	69.72
Germanium	DC A4	5.656			20°C	2.450	Ge^{+2} 0.93	5.32	32	72.59
Ge							Ge^{+4} 0.53			
Gold	FCC A1	4.079			20°C	2.88	Au^{+} (1.37)	19.3	79	196.97
Hafnium	HCP A3	3.194		5.051	20°C	3.15	HF^{+4} 0.81	13.1	72	178.49
Holmium	HCP A3	3.577		5.616	20°C	3.487	HO^{+3} 0.97	8.80	67	164.93
Illinium (Promethium)										
Indium	FC Tet. A6	4.598		4.947	20°C	3.25	In^{+3} 0.81	7.31	49	114.82
Iodine	Orthorhombic	4.787	7.266	9.793	20°C	2.71	I^{+7} 0.50	4.94	53	126.90
Iridium	FCC A1	3.839			20°C	2.714	Ir^{+4} 0.66	22.5	77	192.20
* Iron α	BCC A2	2.866			20°C	2.48	Fe^{+2} 0.76	7.86	26	55.85
Iron γ	FCC A1	3.571			20°C	2.53	Fe^{+3} 0.64			
Iron γ	FCC A1	3.647			950°C	2.585				
* Lanthanum α	HCP A3	3.770		12.16	20°C	3.74	La^{+3} 1.15	6.17	57	138.9
Lanthanum β	FCC A1	5.296			20°C	3.762				
Lead	FCC A1	4.95			20°C	3.5	Pb^{+2} 1.20	11.4	82	207.19
Pb							Pb^{+4} 0.84			
* Lithium	BCC A2	3.509			20°C	3.039	Li^{+1} 0.60	0.53	3	6.94
Coldworked	FCC A1	4.40			-195°C	3.11				
Lutecium	HCP A3	3.503		5.55	20°C	3.45	Lu^{+3} 0.93	9.84	71	174.97
Magnesium	HCP A3	3.209		5.21	20°C	3.196	Mg^{+2} 0.65	1.74	12	24.31

Table C-2. (Cont'd.)

Element	Structure	Lattice Constant <i>a</i>	<i>b</i>	<i>c</i> or Axial Angle	Temperature	Closest Distance	Ionic Radii	Density	Atomic Number	Weight
* Manganese α	Cubic A12	8.914			20°C	2.24	Mn $^{+2}$ 0.80	7.43	25	54.94
Manganese β	Cubic A13	6.314			20°C	2.37	Mn $^{+4}$ 0.52			
Manganese γ	FCC A1	3.812			20°C	2.69	Mn $^{+7}$ (0.46)			
Mercury	Rhombo. A10	3.005		70°31.7'	-46°C	3.006	Hg $^{+1}$ —	13.6	80	200.59
							Hg $^{+2}$ 1.10			
Molybdenum	BCC A2	3.147			20°C	2.725	Mo $^{+4}$ 0.68	10.2	42	95.94
							Mo $^{+6}$ 0.62			
Neodymium	HCP A3	3.658		11.8	20°C	5.90	Nd $^{+3}$ 1.08	7.00	60	144.24
Nickel	FCC A1	3.524			20°C	2.49	Ni $^{+2}$ 0.74	8.9	28	58.7
Niobium	BCC A2	3.301			20°C	2.859	Nb $^{+4}$ 0.67	8.4	41	92.91
							Nb $^{+5}$ (0.70)			
Osmium	HCP A3	2.735		4.319		2.73	Os $^{+4}$ 0.67	22.6	76	190.2
Oxygen							O $^{-2}$ 1.40	1.14	8	16.00
Palladium	FCC A1	3.891			20°C	2.75	Pd $^{+2}$ 0.50	12.0	46	106.4
Platinum	FCC A1	3.924			20°C	2.775	Pt $^{+2}$ 0.52	21.4	78	195.09
							Pt $^{+4}$ 0.56			
Potassium	BCC A2	5.247			20°C	4.55	K $^{+1}$ 1.33	0.86	19	39.10
* Praseodymium α	HCP A3	3.673		5.92	20°C	3.64	Pr $^{+3}$ 1.09	6.77	59	140.91
Praseodymium β	FCC A1	5.151			20°C	3.649	Pr $^{+4}$ 0.92			
Rhenium	HCP A3	2.761		4.458	20°C	2.74		21.0	75	186.2
* Rhodium β	FCC A1	3.803			20°C	2.689	Rh $^{+3}$ 0.75	12.4	45	102.91
							Rh $^{+4}$ 0.65			
Rubidium	BCC A2	5.70			20°C	4.93	Rb $^{+1}$ 1.48	1.53	37	85.47
* Scandium α	FCC A1	4.541			20°C	3.21	Sc $^{+3}$ 0.81	3.0	21	44.96
Scandium β	HCP A3	3.31		5.273	20°C	3.24				
* Selenium	Hex. A8	4.366		4.959	20°C	2.32	Se $^{+6}$ 0.42	4.79	34	78.96
Silicon	DC A4	5.4308			20°C	2.35	Si $^{+4}$ 0.41	2.33	14	28.09
Silver	FCC A1	4.086			20°C	2.89	Ag $^{+1}$ 1.26	10.5	47	107.87
Sodium	BCC A2	4.29			20°C	3.715	Na $^{+1}$ 0.95	0.97	11	22.99

Table C-2 (Cont'd.)

Element	Structure	Lattice Constant <i>a</i>	<i>b</i>	<i>c</i> or Axial Angle	Temperature	Closest Distance	Ionic Radii	Density	Atomic Number	Weight
Strontium	FCC A1	6.085			20°C	4.31	Sr $^{+2}$ 1.13	2.6	38	87.62
* Sulfur α	Orthorhombic	10.5	12.94	24.6	20°C	2.45	S $^{+6}$ 0.29	2.07	16	32.06
							S $^{-2}$ 1.84			
Tantalum	BCC A2	3.298			20°C	2.86	Ta $^{+6}$ 0.73	16.6	73	180.95
Technetium	HCP A3	2.735		4.388		2.735		11.5	43	99
Tellurium	Hex. A8	4.457		5.927	20°C	2.87	Te $^{+4}$ 0.84	6.24	52	127.6
							Te $^{+6}$ (0.56)			
							Te $^{-2}$ 2.21			
Terbium	HCP A3	3.601		5.694	20°C	3.52	Tb $^{+3}$ 1.00	8.27	65	158.92
* Thallium α	HCP A3	3.457		5.525	20°C	3.41	Tl $^{+1}$ 1.40	11.85	81	204.37
							Tl $^{+3}$ (0.95)			
Thorium	FCC A1	5.084			20°C	3.60	Th $^{+4}$ 0.95	11.7	90	232.04
Thulium	HCP A3	3.54		5.555	20°C	3.45	Tm $^{+3}$ 0.95	9.33	69	168.93
Tin α (gray)	DC A4	6.892			18°C	2.98	Sn $^{+2}$ 1.12	7.30	50	118.64
* Tin β (white)	Tet. A5	5.831		3.181	20°C	3.02	Sn $^{+4}$ 0.71			
* Titanium α	HCP A3	2.951		4.683	25°C	2.89	Ti $^{+2}$ 0.90	4.51	22	47.90
Titanium β	BCC A2	3.306			900°C	2.89	Ti $^{+3}$ 0.70			
							Ti $^{+4}$ 0.68			
* Tungsten α	BCC A2	3.165			20°C	2.75	W $^{+4}$ 0.64	19.3	74	183.85
							W $^{+6}$ 0.68			
* Uranium α	Orthorhombic	2.858	5.877	4.955	20°C	2.77	U $^{+4}$ 0.89	19.07	92	238.04
Vanadium	BCC A2	3.028			30°C	2.63	V $^{+3}$ 0.74	6.1	23	50.94
							V $^{+4}$ 0.57			
							V $^{+5}$ (0.59)			
Ytterbium	FCC A1	5.486			20°C	3.86	Yb $^{+2}$ 1.13	6.98	70	173.04
Yttrium	HCP A3	3.647		5.731	20°C	3.58	Y $^{+3}$ 0.93	4.47	39	88.91
Zinc	HCP A3	2.665		4.947	20°C	2.66	Zn $^{+2}$ 0.74	7.14	30	65.37
* Zirconium α	HCP A3	3.231		5.148	20°C	3.17	Zr $^{+4}$ 0.80	6.49	40	91.22
* Zirconium β	BCC A2	3.609			867°C	3.13				